Liquid-Phase Hydrogenation of Cinnamaldehyde over a Ru−Sn Sol−Gel Catalyst. 1. Evaluation of Mass Transfer via a Combined Experimental/Theoretical Approach

ARTICLE *in* INDUSTRIAL & ENGINEERING CHEMISTRY RESEARCH · APRIL 2004

Impact Factor: 2.59 · DOI: 10.1021/ie0340802

2 AUTHORS, INCLUDING:

Dmitry Murzin
Åbo Akademi University
430 PUBLICATIONS **6,190** CITATIONS

Liquid-Phase Hydrogenation of Cinnamaldehyde over a Ru−Sn Sol−Gel Catalyst. 1. Evaluation of Mass Transfer via a Combined Experimental/Theoretical Approach

Jan Hájek and Dmitry Yu. Murzin*

Laboratory of Industrial Chemistry, Process Chemistry Centre, Åbo Akademi University, Biskopsgatan 8, FIN-20500 Turku/Åbo, Finland

Hydrogenation of cinnamaldehyde over a 5% Ru−5% Sn/SiO_2 sol−gel catalyst was investigated in a stirred batch reactor. A combined experimental/theoretical approach was used to elucidate the impact of gas/liquid, liquid/solid, and pore diffusion. To determine the kinetic region area, the catalytic performance at different reaction conditions was evaluated. The complex evaluation presented comprises all important factors such as catalyst mass, stirring speed, liquid load, catalyst particle size, etc., that might contribute to mass-transfer limitations. Theoretical calculations were confirmed by experimental results showing its applicability.

Introduction

Application of heterogeneous catalytic reactions in the production of fine chemicals is of increasing interest. Such reactions are often carried out in batch and semibatch reactors.

There are various experimental procedures and theoretical criteria to confirm the assumption of a kinetic region.[1−4] In the application of these diagnostic criteria, however, exist several limitations.

In the case of three-phase heterogeneous catalytic reactions, the rate of process and its selectivity can be determined either by intrinsic reaction kinetics or by external diffusion (on the gas/liquid and gas/solid interface) as well as by internal diffusion through the catalyst pores. Careful analysis of mass transfer is important for the elucidation of intrinsic catalytic properties, for the design of catalysts, and for the scale-up of processes.

Nevertheless, in scale-up the operating conditions are selected in a way that the process is shifted from the kinetic region to a diffusionally controlled one. That is why it is of utmost importance to know how the shift will affect not only the conversion but also the selectivity.

In the present study, the influence of mass transfer in the liquid-phase hydrogenation of cinnamaldehyde was studied.

Selective preparation of unsaturated alcohols from corresponding unsaturated carbonyl compounds is an important step in the preparation of various fine chemicals.[5−7] The reaction is even more challenging because the reduction of the C=O double bond is thermodynamically restricted. Despite the fact that high yields of the desired unsaturated alcohols can be achieved by using inorganic reducing agents,[8−10] economic constraints of these conventional methods make heterogeneous catalysis more attractive.

In particular, a fairly good intrinsic selectivity toward unsaturated alcohols was observed for ruthenium catalysts.[11,12] The selectivity of ruthenium catalysts can be further improved by the addition of a second metal such as Fe, Ge, Pb, or Zn.[13−18] In hydrogenation of cinnamaldehyde, promising yields of unsaturated alcohols have been obtained with tin-promoted ruthenium catalysts.[19,20] The sol−gel procedure, with respect to the preparation of supported bimetallic catalysts, allows synthesis of bimetallic catalysts with a homogeneous distribution of finely dispersed metals.[21,22] Other advantages include improved thermal stability of metals, higher surface areas, well-defined pore-size distribution, and the ability to control the microstructure of the carrier.[23,24]

This work is devoted to hydrogenation of cinnamaldehyde over a sol−gel Ru−Sn/SiO_2 catalyst in a stirred batch reactor. In the previous contributions,[25,26] the influence of the catalyst reduction mode on the properties of sol−gel Ru−Sn/SiO_2 catalysts was reported (with special attention on the characterization of prepared catalysts).

In the present paper, the main attention is focused on the elucidation of the impact of mass transfer. In part 2 of this series of papers, kinetic modeling will be addressed.

Experimental Section

Sol−Gel 5% Ru−5% Sn/SiO_2 Catalyst. Pertinent amounts of ruthenium [$RuCl_3 \cdot xH_2O$ ($x \leq 1$), Aldrich] and a tin precursor ($SnCl_2$, Aldrich) were dissolved in 18 mL of ethanediol. The acquired solution was stirred for 30 min at 343 K. Consequently, a support precursor [98% $Si(OC_2H_5)_4$, Aldrich] was added to the cooled solution of metal salts, and the mixture was heated to 343 K. After 3 h of stirring, distilled water (90 mL) was added, and stirring followed at 343 K until a gel was formed. The obtained gel was left for 12 h and then dried. To remove low-boiling residues, the first drying stage was performed in a vacuum water-rotary evaporator. The bath temperature was slowly increased (20 K/h, 1.9 kPa) up to 363 K, and the final temperature was kept for 12 h. The second drying step was performed in an oil bath (0.5 kPa) at 473 K for 2 h. The obtained catalyst was reduced by a 10% solution of $NaBH_4$ (97%, Fluka) in

* To whom correspondence should be addressed. Tel.: +358-2-215-4985. Fax: +358-2-215-4479. E-mail: Dmitry.Murzin@abo.fi.

10.1021/ie0340802 CCC: $27.50
Published on Web 04/03/2004

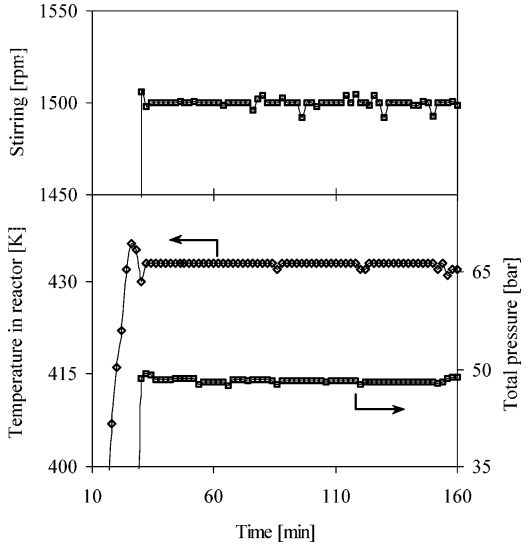

Figure 1. Reactor temperature, pressure, and stirring rate profiles (433 K, 48 bar, 1500 rpm).

Table 1. Reactor Specifications

manufacturer	Autoclave Engineers
type	EZE−SEAL
nominal reactor volume	500 mL
material	316 stainless steel
max allowable pressure	227 bar
max design metal temperature	727 K
min design metal temperature	253 K
agitator	dispersion turbine
max agitation rate	2300 rpm
seal material	metal gasket
heating	1000 W heating mantle

distilled water and carefully washed with small amounts (10−20 mL) of distilled water and ethanol (ca. 500 mL). The washed catalyst was dried in a nitrogen (5.0) atmosphere (2 h, 473 K).

The pore-size distribution (Dollimore-Heal) and Brunauer−Emmett−Teller surface area of the prepared 5% Ru−5% Sn/SiO_2 catalyst were determined from full nitrogen adsorption−desorption isotherms (Sorptomatic 1900, Carlo Erba Instruments). The catalyst had a mesoporous structure with a narrow distribution of pores (1−4 nm), and the surface area was 297 m^2/g. The ruthenium and tin contents were verified by DCP (direct current plasma).

Catalytic Experiments. Hydrogenations were carried out in 2-propanol in a stirred batch reactor (Table 1). The catalyst was ex situ activated under a hydrogen (5.0) flow for 2 h (473 K, 30 mL/min) prior to the reaction. The amount of cinnamaldehyde charged in the reactor was invariable (3 g) in all experiments. Samples collected during the reaction were analyzed with a HP-5890 Series II Plus gas chromatograph (GC; Hewlett-Packard). The GC was equipped with a flame ionization detector and a capillary column (HP 20M). The contents of the individual components in the reaction mixture were determined by the Internal Standardization Method (*n*-decane, Aldrich). The reaction products were identified with GC−MS.

The autoclave used was equipped with automatic flow, pressure, stirring, and temperature control units. Temperature, total pressure in the reactor, and stirring rate profiles were recorded during runs (Figure 1).

Reaction Details. Catalyst activities were evaluated from the initial reaction rates according to the differential method, assuming zero reaction order at the very beginning of the reaction (5 min). The selectivity was calculated as the molar ratio of the product to the total formed at the conversion of 50%.

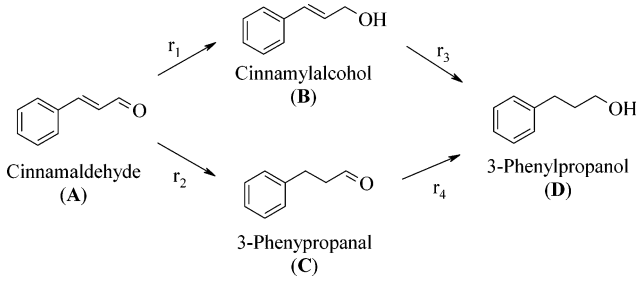

Figure 2. Cinnamaldehyde hydrogenation network.

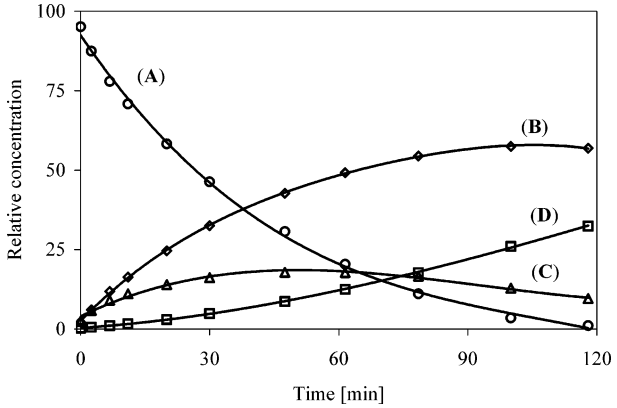

Figure 3. Typical hydrogenation of cinnamaldehyde (0.5 g_{cat}, 433 K, 70 bar).

Typical main reaction products were cinnamyl alcohol (**B**), 3-phenylpropanal (**C**), and 3-phenylpropanol (**D**). Reactions followed the reaction scheme presented in Figure 2. Partial hydrogenation of the aromatic ring was observed during experiments at the highest temperature (483 K).

A typical hydrogenation run is presented in Figure 3.

The kinetic pattern demonstrated follows the general behavior characteristic for parallel-consecutive reactions (Figure 2). The selectivity toward the desired compound in such a network can be affected by mass transport limitations, particularly if the reaction order of the desired reaction (r_1) is different compared to the reaction order of a parallel reaction (r_2).

Results and Discussion

The examination of the mass-transfer influence is significantly important in the case of multiphase reaction systems because quite often mass-transfer limitations appear at industrial conditions. The reaction system is free of transfer limitations in the so-called "kinetic" region if the rate of all transfer processes is higher than the rate of the chemical reaction.

In the case of three-phase catalytic hydrogenation, the following mass-transfer processes should be considered (Figure 4): gas/liquid mass transfer, transport of the dissolved gas and dissolved reactants (and products) from the liquid bulk to the outer surface and from the outer surface of the catalyst particles (external diffusion limitation), and transport inside the solid particles (internal diffusion). All of these processes might influence the overall reaction rate and reaction selectivity.

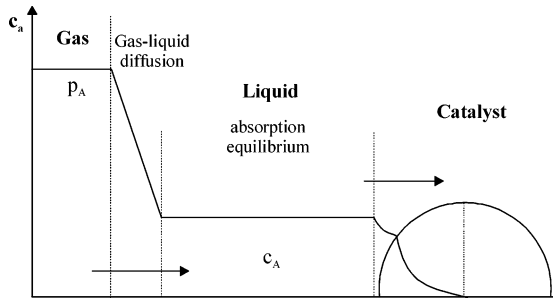

Figure 4. Schematic view of the mass-transfer processes in three-phase hydrogenations.

To evaluate the possible mass-transfer limitations, a calculation procedure and experimental approach will be discussed.

Gas/Liquid Mass Transfer and External Mass Transfer. (a) Calculation of the Mass-Transfer Coefficient. The mass-transfer processes (film diffusion and external diffusion) are determined mainly by the mass-transfer coefficient β. Different methods can be used to calculate the mass-transfer coefficient. The starting point in the treatment presented below is the relationship between dimensionless numbers.

$$Sh = f(Re,Sc) \tag{1}$$

The dependence of the *Re* number on the local velocity can be established in terms of the Kolmogorov theory of turbulence.[27] According to this theory, the only parameter needed to describe the probability distribution of the relative velocity field V_λ in a homogeneous isotropic turbulent fluid is the average energy dissipation ϵ, i.e.,

$$V_\lambda \propto (\epsilon\lambda)^{1/3} \tag{2}$$

leading to

$$Re_d \propto (\epsilon d/\nu^3)^{1/3} \tag{3}$$

Collected experimental data for slurry reactors[28] demonstrated that the relation in eq 1 can be described by the following equation:

$$Sh = 1.0Re^{1/2}Sc^{1/3} \tag{4}$$

Equation 4 provides a possibility of estimating the gas/liquid and liquid/solid mass-transfer coefficients β_{GL} and β_{LS} according to

$$\beta_{GL} = (\epsilon D^4\rho/\eta {d_{bu}}^2)^{1/6} \tag{5}$$

and

$$\beta_{LS} = (\epsilon D^4\rho/\eta {d_p}^2)^{1/6} \tag{6}$$

where ϵ denotes the specific mixing power, $D_{AB}°$ is the mutual diffusion coefficient of solute A in solvent B, ρ is the solvent density, η is the solvent viscosity, d_{bu} is the diameter of the gas bubbles, and d_p is the diameter of the catalyst particles.

Equation 5 was in the present study applied for the calculations of the gas/liquid mass-transfer coefficient.[29] Analogously, eq 6 was used for the calculation of mass transfer through a liquid/solid interface.[30]

(b) Calculation of the Specific Mixing Power. The specific mixing power (dissipation energy ϵ) in eqs 5 and 6 was calculated at different stirring rates and liquid loads by measuring the dissolution rates of benzoic acid (BA; 99%, Aldrich).

The rate of BA dissolution (pellets, $m = 1$ g) in distilled water was measured at atmospheric pressure. The amount of dissolved acid in collected samples was determined by potentiometric titration with 0.2 M NaOH (751 GPD Titrino, Metrohm Ltd., Herisau, Switzerland). The mass-transfer coefficient during dissolution was calculated according to

$$\beta = cV_L/S_{BA}c_{av}\tau \quad \text{(m/s)} \tag{7}$$

where S_{BA} denotes the overall surface of solid particles of BA and c_{av} is the average concentration at time τ. The actual solute concentration is c, and V_L is the liquid-phase volume in the reactor.[29] The average BA concentration at time τ is obtained from

$$c_{av} = \frac{c}{\ln\left(\frac{c_{eq}}{c_{eq} - c}\right)} \quad \text{(g/cm}^3\text{)} \tag{8}$$

Experimentally determined values of mass-transfer coefficients obtained from BA dissolution are consequently used for the calculation of ϵ:

$$\epsilon^{1/6} = \frac{\beta {d_p}^{1/3}}{D^{2/3}}\left(\frac{\eta}{\rho}\right)^{1/6} \quad [\text{(W/kg)}^{1/6}] \tag{9}$$

The particle diameter d_p was approximated by the diameter of the ball-shaped particles having the same surface area as that of the pellets used. To achieve a negligible decrease of the external surface area of the pellets during dissolution, a high excess of solute was used (dissolution of 10 wt % of inserted pellets resulted in the equilibrium BA concentration).

For the temperature 293 K, the diffusion coefficient $D_{AB}°$ of BA in water (in eq 9) was calculated from a modified Tyn−Calus method (ref 31, p 600) taking into account the water density ($\rho = 998$ kg/m^3) and viscosity ($\eta = 10^{-3}$ N·s/m^2).

$$D_{AB}° = 8.93 \times 10^{-8}\frac{{V_{b(B)}}^{0.267}}{{V_{b(A)}}^{0.433}}\frac{T}{\eta_B}\left(\frac{\sigma_B}{\sigma_A}\right)^{0.15} \quad \text{(cm}^2\text{/s)} \tag{10}$$

The volumes at boiling points $V_{b(A)}$ and $V_{b(B)}$ were obtained from the Yamada and Gunn modification of the Rackett equation (ref 32, p 4.35):

$$V_b = V_c(0.29056 - 0.08775\omega)^{(1-T_b/T_c)^{2/7}} \tag{11}$$

where V_c is the critical volume, ω the acentric factor, T_b the normal boiling temperature, and T_c the critical temperature. Using the property databank,[31] values $V_{b(A)} = 19.527$ cm^3/mol and $V_{b(B)} = 105.108$ cm^3/mol were obtained. A comparison of the calculated (0.922 g/cm^3) and tabulated (0.958 g/cm^3) water density V_A at its normal boiling point gives an estimation error of −3.8%.

The surface tension of solvent A (water) is $\sigma_A = 72.8$ dyn/cm at 293 K. For solute B (BA), the Macleod−Sugden correlation (ref 31, p 633) is used:

$$\sigma^{1/4} = p(\rho_L - \rho_V) \tag{12}$$

Table 2. Dissipation Energy Obtained at 1500 rpm at Various Liquid Volumes

volume [mL]	$\beta \times 10^{-5}$ [m/s]	$\epsilon^{1/6}$ [(W/kg)$^{1/6}$]
400	6.6	2.03
300	6.8	2.00
200	2.5	0.77
150	3.3	0.80

Table 3. Dissipation Energy Obtained at a Liquid Volume of 200 mL at Various Stirring Rates

agitation [rpm]	$\beta \times 10^{-5}$ [m/s][a]	$\epsilon^{1/6}$ [(W/kg)$^{1/6}$][a]
2300	2.5	0.83
1500	2.3	0.77
800	3.6	1.18
400	3.0	0.99
150	1.3	0.43

[a] $\epsilon_{max}^{1/6} = 3.11$ (W/kg)$^{1/6}$.

The experimental temperature was well below the boiling point of BA; thus, its vapor density ρ_V is much smaller than ρ_L (1.316 g/cm^3), where ρ_L is its liquid density. Parachor p was estimated from Quayle functional group contributions: $p = C_6H_5 + -COOH = 189.6 + 73.8 = 263.4$. Application of eq 12 leads to $\sigma_B = 64.9$ dyn/cm. Consequently, the ratio $(\sigma_B/\sigma_A)^{0.15} = 1.017 \approx 1$; therefore, eq 10 might be further approximated by

$$D_{AB}^{\circ} = 8.93 \times 10^{-8} \frac{V_{b(B)}^{0.267}}{V_{b(A)}^{0.433}} \frac{T}{\eta_B} \qquad (13)$$

The viscosity of water η at 293 K is 1 cP (i.e., 10^{-3} Pa·s). Then the value of the diffusion coefficient of BA at atmospheric pressure is $D_{AB}^{\circ} = 7.7 \times 10^{-10}$ m^2/s (293 K).

The power of the motor used for stirring was $W = 186.4$ W; the maximum energy dissipation of the motor used for mixing is given by

$$\epsilon_{max} = W/m \qquad (14)$$

where m is the mass of the suspension.[29] It follows from the experiments with BA that typically only a very small fraction of the motor power was used for stirring (Tables 2 and 3).

(c) Gas/Liquid Mass Transfer. The rate of hydrogen dissolution I is determined by the mass transfer according to a following equation:

$$I = \beta_{GL} F (c_{eq} - c_L) \quad \text{(mol/s)} \qquad (15)$$

where β_{GL} is the coefficient of mass transfer through the gas film into the bulk liquid phase (often denoted as k_L), F is the gas/liquid interfacial area, c_{eq} is the equilibrium hydrogen concentration, obtained from hydrogen solubility data, and c_L is its actual concentration in the liquid phase.[33]

The value of the mass-transfer coefficient obtained from the experimental reaction rate (70 bar, 373 K) compared to the value of the mass transfer that might be attained as a result of energy dissipated by the stirrer demonstrates the impact of gas/liquid mass transfer.

The maximum rate of dissolution corresponds to the case where c_L is essentially smaller than c_{eq}; i.e., assuming $c_{eq} \gg c_L$, one arrives at

$$I = \beta_{GL} F c_{eq} \qquad (16)$$

The mass-transfer coefficient β_{GL} was calculated from the experimentally obtained value of dissipation energy ϵ according to eq 5.

For the estimation of D_{AB}°, the Wilke−Chang equation was used. This equation gives accurate results in the prediction of diffusion coefficients of gases in liquids (ref 31, p 598):

$$D_{AB}^{\circ} = \frac{7.4 \times 10^{-8} (\phi M_B)^{1/2} T}{\eta_B V_{b(A)}^{0.6}} \quad \text{(cm}^2\text{/s)} \qquad (17)$$

The dimensionless association factor ϕ is taken as 1.4 for 2-propanol, M_B is the molecular weight of the solvent (60 g/mol), η_B is the solvent viscosity (in cP) at temperature T (K), and $V_{b(A)}$ is the liquid molar volume at the solute's normal boiling point (in cm^3/mol).

Estimation of the solvent viscosity η_B at temperatures $T_r > 0.7$ (reduced temperature T_r is defined by T/T_c, and the critical temperature T_c of 2-propanol is 508.3 K) was based on the Sastri method (ref 32, p 9.75):

$$\ln \eta_{SR} = \left[\frac{\ln \eta_b}{\ln(a\eta_b)}\right]^{\kappa} \ln(a\eta_b) \quad \text{(mPa·s)} \qquad (18)$$

where η_b is the viscosity at normal boiling point temperature and $a = 0.1175$ for alcohols. Viscosity η_b was calculated from the Sastri−Rao method (ref 32, p 9.61) by applying functional group contributions where the number of carbon atoms C is equal to 3:

$$\eta_b = CH_3- + -CH- + -OH + -CH_3 = 0.105 - 0.110 + 0.615 - 0.092C + 0.004C^2 - 10^{-0.58C} + 0.105 = 0.457 \text{ mPa·s} = 457\ \mu\text{Pa·s}$$

Parameter κ in eq 18 is defined as $\kappa = (T_c - T)/(T_c - T_b)$, where T_b is the normal boiling point temperature (355.39 K). Applying the numerical values reported above, one arrives at $\eta_{SR} = 0.340$ cP (373 K, 1 bar). The pressure effect on viscosity was estimated from the Lucas method (ref 31, p 436):

$$\frac{\eta}{\eta_{SR}} = \frac{1 + d'(\Delta P_r/2.118)^{a'}}{1 + c'\omega\Delta P_r} \qquad (19)$$

where $\Delta P_r = (P - P_{vp})/P_c$; values of P_{vp} and P_c are taken from the Effect of the Liquid Load section. The empirical parameters are defined in the following way:

$$d' = 0.3257/(1.0039 - T_r^{2.573})^{0.2906} - 0.2086$$

$$a' = 0.9991 - 4.674 \times 10^{-4}/(1.0523 T_r^{-0.03877} - 1.0513)$$

$$c' = -0.07921 + 2.1616 T_r - 13.4040 T_r^2 + 44.1706 T_r^3 - 84.8291 T_r^4 + 96.1209 T_r^5 - 59.8127 T_r^6 + 15.6719 T_r^7$$

Calculation of the 2-propanol viscosity then gives $\eta_B = 0.427$ cP under the total pressure of 70 bar at 373 K.

Hydrogen molar volume $V_{b(A)}$ at its normal boiling point was calculated according to eq 11, where $\omega = -0.217$, $V_c = 65$ cm^3/mol, $T_b = 20.38$ K, and $T_c = 33.25$ K. The value $V_{b(A)} = 9.862$ cm^3/mol was obtained.

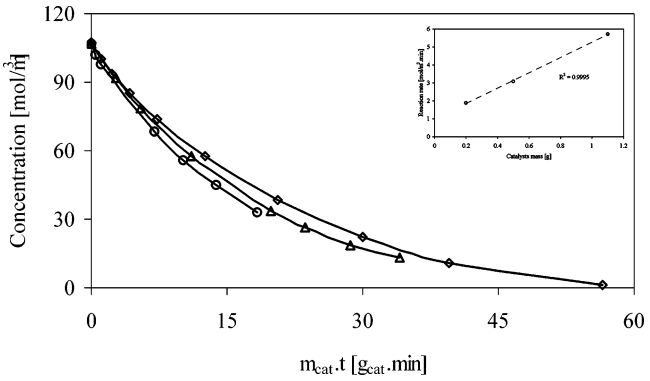

Figure 5. Cinnamaldehyde hydrogenation for 0.2 (○), 0.5 (◇), and 1.1 (△) g of catalyst (433 K, 70 bar).

Consequently, the value of the hydrogen diffusion coefficient in 2-propanol is $D_{AB}° = 1.5 \times 10^{-8}$ m^2/s (373 K, 70 bar).

The experimentally obtained dissipation energy $\epsilon^{1/6} = 0.77$ (W/kg)$^{1/6}$ (1500 rpm, 200 mL), 2-propanol density (the calculation procedure is elaborated on in the following section) $\rho = 705$ kg/m^3, and its viscosity $\eta = 0.427$ cP $= 4.27 \times 10^{-4}$ N·s/m^2 (373 K, 70 bar). The diameter of the hydrogen bubbles was taken as $d_{bu} = 0.15$ cm $= 1.5 \times 10^{-3}$ m. Calculation gave the value of gas/liquid mass-transfer coefficient $\beta_{GL} = 5.44 \times 10^{-4}$ m/s.

The rate of gas dissolution is determined by the gas/liquid interfacial area F. Its ratio to the liquid-phase volume V_L in the reactor is

$$\frac{F}{V_L} = \frac{6\Phi_G}{d_{bu}} \tag{20}$$

where Φ_G is the gas volume fraction in the suspension; Φ_G is always ≤ 0.4.[34] The initial liquid-phase volume was 200 cm^3. Taking into account the volume of the liquid phase at reaction conditions 228 cm^3 (the calculation procedure is elaborated on in the following section) and $\Phi_G = 0.01$, the diameter of the hydrogen bubbles $d_{bu} = 0.15$ cm and the obtained value of F is 91 cm^2. The equilibrium concentration of hydrogen in 2-propanol[35] at reaction conditions of 373 K and 70 bar is $c_{eq} \approx 3.27 \times 10^{-4}$ mol/cm^3. Consequently, the calculated value of the maximum dissolution rate is $I = 6.6 \times 10^{-4}$ mol/s.

The measured initial hydrogenation rate at 373 K and 70 bar was 3.25×10^{-6} mol/s (catalyst mass 0.5 g); thus, it can be concluded that hydrogen dissolution was orders of magnitude higher than the rate of hydrogen consumption. Apparently, the reaction was not mass-transfer-limited on the gas/liquid interface.

An alternative experimental way to estimate the influence of film diffusion on the gas/liquid interface is to perform experiments with different catalyst masses. Plots of the substrate concentration vs normalized catalyst mass displayed in Figure 5 indicate that gas/liquid mass-transfer resistance does not play a significant role at the experimental conditions tested.

The plotted normalized cinnamaldehyde concentration−time curves for different catalyst masses coincide (Figure 5), clearly showing that gas/liquid diffusion can be neglected.

(d) External Mass Transfer. The external diffusion limitation (mass transfer through a liquid/solid interface) is determined by the diffusion rate of the reactant to the external surface or out from the catalyst particles surface for the product diffusion, respectively. The substance flow J to the external surface is defined by

$$J = \beta_{LS} S_{cat} (c_L - c_S) \tag{21}$$

where β_{LS} is the coefficient of mass transfer through the liquid film around the catalyst particle, S_{cat} is the external surface area of the catalyst particles, c_L is the hydrogen concentration in the bulk liquid, and c_S is its concentration on the catalyst surface.[27] In the kinetic region, $c_L \approx c_S$; thus, $c_L - c_S \rightarrow 0$.

The experimentally obtained rate of hydrogen consumption was 3.25×10^{-6} mol/s (373 K, 70 bar). For calculation of the mass-transfer coefficient in the case of 200 cm^3 solvent load, $\epsilon^{1/6} = 0.77$ (W/kg)$^{1/6}$ is acquired from the dissolution of BA; $D_{AB}°$, ρ, and η (373 K, 70 bar) are listed above. Considering spherical particles ($d_p = 4.5 \times 10^{-3}$ cm) of density $\rho_{cat} = 0.75$ g/cm^3, the mass transfer through a liquid/solid is $\beta_{LS} = 1.53 \times 10^{-3}$ m/s and the external surface area of the catalyst is $S = 889$ cm^2 (0.5 g$_{cat}$).

Calculations give a negligible hydrogen concentration difference between the liquid bulk and particle surface $c_L - c_S = 2.39 \times 10^{-8}$ mol/cm^3. Comparing this value with the value of hydrogen solubility, one arrives at an evident conclusion that liquid film diffusion does not limit the reaction rate.

(e) Gas/Liquid and Liquid/Solid Diffusion. Experimental Approach. Following eqs 5 and 6, the mass-transfer coefficient depends on the energy dissipation. The latter is a function of the mixing power, related to the stirring speed according to

$$W \propto n^3 \tag{22}$$

where n is the stirring speed. When eqs 5, 9, and 14 are combined, the dependence of the mass-transfer coefficient on the stirring speed can be established as

$$\beta \propto n^{1/2} \tag{23}$$

It follows from eqs 5 and 6 that the rate of mass transfer through the gas/liquid as well as liquid/solid interface depends on hydrodynamic conditions in the slurry reactor, frankly on the agitation efficiency (which, in turn, is influenced by the selection of solvent, stirring rate, liquid volume, and design of the reactor internals).

(f) Dependence of the Reaction Rate on the Stirring Speed. As is commonly known, agitation in three-phase reactors is of great importance, pledging the high mass-transfer efficiency. Varying the stirring rates is a standard test to determine and eliminate gas/liquid and liquid/solid mass-transport limitation. The reaction is free from mass-transfer limitation when changes in agitation do not result in changes of the reaction rates.[36]

In the present study, the dependence of the catalyst activity on agitation was evaluated at different stirring rates with a 200 mL solvent volume (Table 4). The

Table 4. Activity−Stirring Rate Dependence (433 K, 70 bar)

agitation [rpm]	initial activity [mol × 10^{-4}/min·g$_{cat}$]	selectivity [%]	$\beta \times 10^{-5}$ [m/s]	$\epsilon^{1/6}$ [(W/kg)$^{1/6}$]
2300	12.3	63	2.5	0.83
1500	12.8	60	2.5	0.77
150	11.3	60	1.3	0.43

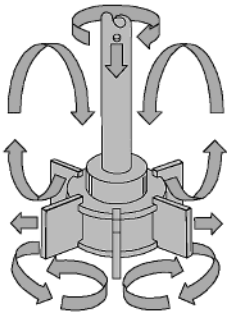

Figure 6. Gas dispersion at 1500 rpm and agitator construction.

Table 5. Activity−Solvent Volume Dependence (1500 rpm, 433 K, 70 bar)

	initial solvent volume [mL]			
	400	300	200	150
initial reactor filling [%]	67	50	33	25
activity [mol × 10^{-4}/min·g_{cat}]	6.7	12.2	11.4	11.4

values of mass-transfer coefficients were evaluated from the data of BA dissolution.

It is interesting to note that even at low stirring rates (150 rpm) the catalytic activity was comparable to the activity obtained at much higher rpm values, indicating the high stirring efficiency of the dispersion turbine used (Figure 6). To be more illustrative and better visible, the photograph in Figure 6 was colored to show the gas in red.

The gas is not spread homogeneously within the liquid as a result of the intrinsic properties of the stirrer. Although the dispersion turbine type stirrer shown spreads gas, it is not that efficient in providing homogeneous gas dispersion in the whole liquid phase. Note that conventional stirrers usually do not spread the gas, and only vortexes are visible. In any case, dispersion turbines are providing the increased liquid/surface interface, thus facilitating gas dissolution and increasing the stirring efficiency.

Results presented in Table 4 show the apparent danger of establishing the kinetic region based just on the results of catalytic experiments at different stirring speeds. The catalytic activity independent of rpm could be explained simply by the fact that a higher agitator speed does not influence the specific mixing power, as is clearly seen from Table 4. Therefore, experimental verification of the absence of mass transfer should be combined with calculations in the way as presented in previous sections.

(g) Effect of the Liquid Load. Experiments at different solvent volumes were performed at a stirring rate of 1500 rpm (Table 5). The reaction rate was strongly effected (decreased) by the initial liquid volume after the reactor was overfilled (400 mL). On the other hand, withdrawal of the samples at 150 mL solvent volume was problematic, because of the sampling tube end position above the reactor bottom.

The estimated solvent volume in the reactor at different reaction conditions was calculated for safety reasons and to explain the observed dependence.

Considering the mass fraction of the substrate in solvent to be negligible (ca. 2 wt %), the estimation of the compressed saturated pure 2-propanol liquid volume at different pressures and temperatures was based on the extended Hankinson−Brobst−Thompson method (ref 31, p 66):

$$V = V_s\left(1 - c'' \ln \frac{b'' + P}{b'' + P_{vp}}\right) \tag{24}$$

Parameters c'' and b'' are obtained from

$$b''/P_c = -1 + a'''(1 - T_r)^{1/3} + b'''(1 - T_r)^{2/3} + d'''(1 - T_r) + e'''(1 - T_r)^{4/3} \tag{25}$$

$$c'' = j''' + k'''\omega \tag{26}$$

where $e''' = \exp(f''' + g'''\omega + h'''\omega^2)$ and parameters $a'''-k'''$ are (ref 30, p 669) $a''' = -9.070\ 217$, $b''' = 62.45326$, $d''' = -135.1102$, $f''' = 4.795\ 94$, $g''' = 0.250047$, $h''' = 1.14188$, $j''' = 0.0861488$, and $k''' = 0.0344483$. The value of acentric factor ω in the expressions of c'' *and* e''' is 0.6637.

Saturated liquid volume V_s was estimated by the Hankinson−Thompson correlation (ref 31, p 55):

$$V_s/V^* = V_R^{(0)}[1 - \varpi_{SRK}V_R^{(\delta)}] \tag{27}$$

The value of the pure-component characteristic volume constant V^* for 2-propanol is 231.3 cm^3/mol. Variables $V_R^{(0)}$ ($0.25 < T_r < 0.95$) and $V_R^{(\delta)}$ ($0.25 < T_r < 1.0$) are functions of T_r:

$$V_R^{(0)} = 1 + a''''(1 - T_r)^{1/3} + b''''(1 - T_r)^{2/3} + c''''(1 - T_r) + d''''(1 - T_r)^{4/3} \tag{28}$$

$$V_R^{(\delta)} = (e'''' + f''''T_r + g''''T_r^{\,2} + h''''T_r^{\,3})/(T_r - 1.00001) \tag{29}$$

Values of T_r for the lowest (373 K) and highest (483 K) reaction temperatures are 0.73 and 0.95, respectively ($T_c = 508.3$ K). Constants in eqs 28 and 29 are $a'''' = -1.52816$, $b'''' = 1.43907$, $c'''' = -0.81446$, $d'''' = 0.190454$, $e'''' = -0.296123$, $f'''' = 0.386914$, $g'''' = -0.0427258$, and $h'''' = -0.0480645$.

For the estimation of reduced vapor pressure P_{vpr}, the Gomez−Thodos (ref 31, p 210) vapor-pressure equation was used.

$$\ln P_{vpr} = \psi\left[\frac{1}{T_r^{\,m^*}} - 1\right] + \iota[T_r^{\,7} - 1] \tag{30}$$

The value of vapor pressure P_{vp} at different temperatures is then calculated from $P_{vp} = P_{vpr}P_c$, where the critical pressure P_c for 2-propanol is 47.6 bar. Parameter ψ is obtained from

$$\psi = \iota/b^* - a^*h^*/b^*$$

Constants ι, a^*, b^*, and h^* are defined by

$$\iota = (2.464/M)\exp(9.8 \times 10^{-6}MT_c) \tag{31}$$

where M (=60 g/mol) is the molar weight of the compound and

$$a^* = (1 - 1/T_{br})/(T_{br}^{\,7} - 1) \tag{32}$$

$$b^* = (1 - 1/T_{br}^{\,m})/(T_{br}^{\,7} - 1) \tag{33}$$

$$h^* = T_{br}[\ln(P_c/1.01325)]/(1 - T_{br}) \tag{34}$$

Table 6. Initial and Calculated Reaction Liquid-Phase Volumes (25 bar)*a*

	reduced temperature			
	0.58	0.73	0.85	0.95
reactor filling [%]	80	90	×	×
	60	67	78	97
	40	45	52	64
	30	34	39	48

[a] Excluding 5% built-in volume.

Table 7. Partial Hydrogen Pressure at Different Reaction Temperatures

total pressure [bar]	373 K	433 K	483 K
25	23	14	x
48	46	37	17
70	68	59	39

where the reduced temperature of normal boiling point T_{br} of 2-propanol is defined as $T_{br} = T_b/T_c$. When the value of T_b is 355.4 K, T_{br} is then 0.7.

Finally, m^* in eqs 30 and 33 is defined by

$$m^* = 0.0052M^{0.29}T_c^{0.72} \tag{35}$$

Estimation of the parameters in the way presented above is valid only for alcohols and water.

The validity of the applied calculation procedure was verified by calculation of the 2-propanol density at normal conditions (1 bar) at room temperature (293 K). The result obtained (0.799 cm^3/g) was ca. 2% higher than the tabulated one (0.785 cm^3/g).

The increase of the liquid volume with temperature is apparent from calculated data as presented in Table 6.

Changes in the solvent volume as a result of increased reaction pressure were almost negligible within in the tested interval of 25−70 bar (max ≈5%). The main reason for the liquid volume increase with temperature is the relatively low critical temperature of 2-propanol (508 K). Taking into account the interval of reaction temperatures (373−483 K) and the estimated solvent volume increase, the selected initial liquid volume for experiments within the kinetic region (part 2) was 200 mL.

A part of the above-presented calculation for the estimation of the solvent vapor pressure can be used consequently for the calculation of the partial hydrogen pressure at different temperatures (Table 7).

When the results in this section are summarized, it can be concluded that the theoretical approach for the estimation of the mass-transfer coefficient is in good agreement with the experimentally obtained results.

Internal Diffusion. The internal mass transfer inside the catalyst particles has been the subject of intensive research since the time that Thiele[37] and Zel'dovich[38] published their seminal papers. Typically, both experimental and theoretical approaches are used in the literature.

The size of the catalyst particles is often mentioned as one of the most important factors influencing the overall rate and selectivity in three-phase catalytic reactions. The experimental results on the impact of the particle size in cinnamaldehyde hydrogenation are presented in Table 8: a decrease in the mean particle size increases both the catalyst activity and selectivity.

Selectivity was affected by internal diffusion. On the basis of the data, the smallest catalyst fraction (≤45 μm)

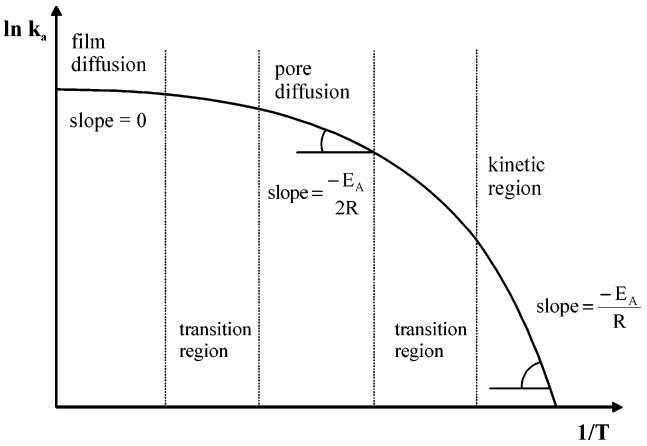

Figure 7. Apparent activation energy in different regions.

Table 8. Influence of the Catalyst Particle Size (433 K, 70 bar)

mean particle size [μm]	particle fraction [μm]	initial activity [mol × 10^{-4}/min·g_{cat}]	selectivity [%]
23	<45	12.3	63
50	<100	11.4	61
54	63−45	11.0	61
95	100−90	8.0	61
165	180−150	7.5	55
750	1000−500	3.7	53

is believed to safely eliminate the influence of internal diffusion. To verify this conclusion, calculation of the catalyst effectiveness factor η_{eff} was performed.

Considering an irreversible reaction of first order on spherical catalyst particles, η_{eff} is determined by the following equation:

$$\eta_{eff} = \frac{3}{\varphi}\left(\frac{1}{\tanh \varphi} - \frac{1}{\varphi}\right) \tag{36}$$

If $\eta_{eff} \rightarrow 1$, the diffusion restriction is negligible. Parameter φ is the Thiele modulus given by

$$\varphi = R\sqrt{k/D_{eff}} \tag{37}$$

where $R = 2.3 \times 10^{-5}$ m is the mean radius of the catalyst particle and the rate constant $k = 7.0 \times 10^{-5}$ s^{-1} was calculated from the reaction rate. The effective diffusion coefficient of hydrogen D_{eff} in 2-propanol is defined as

$$D_{eff} = D\frac{\xi}{\chi} \tag{38}$$

D is the hydrogen diffusion coefficient in the liquid phase (obtained previously), and ξ and χ are the catalyst porosity and tortuosity. Typical values of porosity are in the range of 0.3−0.6; values of tortuosity range from 2 to 5.[39] Assuming $\xi = 0.5$ and $\chi = 3$, the effective diffusion coefficient of hydrogen is $D_{eff} = 2.5 \times 10^{-9}$ m^2/s (373 K, 70 bar).

Calculation of the effectiveness factor under reaction conditions gave $\eta_{eff} \rightarrow 1$, indicating that hydrogen diffusion inside the catalyst pores does not affect the reaction rate.

Temperature Dependence. The rates of chemical processes conducted in the kinetic region are strongly effected by the temperature, while mass transfer significantly decreases the apparent activation energy (Figure 7).

Experimental values of the activation energy above 40 kJ/mol are conventionally assumed for reactions not controlled by mass transfer.[36] An activation energy close to 10 kJ/mol implies a possible mass-transfer limitation. The calculated value of the apparent activation energy[40] in cinnamaldehyde hydrogenation was about 40 kJ/mol, stressing once again the validity of the conclusions that mass transfer did not affect experimental data.

In the part 2 of this series of papers, experimental data for cinnamaldehyde hydrogenation were collected and a detailed analysis of the reaction kinetics was performed. Results of the present paper indicate that the data were obtained without the interference of mass transfer.

Conclusions

To verify the influence of mass transfer in liquid-phase hydrogenation of cinnamaldehyde, a combined theoretical/experimental approach was adopted. Rates of gas/liquid and liquid/solid diffusion were calculated and compared with those experimentally observed. The specific mixing power in the slurry reactor was determined by the measurements of BA dissolution. Conditions at which mass transfer does not influence the reaction were confirmed by the calculation approach and by experimental tests. Evaluation of the effectiveness factor and dependence of the reaction rate on the catalyst particle size showed conditions when pore diffusion is negligible.

Acknowledgment

This work is part of the activities at the Åbo Akademi Process Chemistry Centre within the Academy's of Finland Centre of Excellence Program (2000−2005). The support given by the Graduate School of Chemical Engineering of Finland is also acknowledged.

Notation

$a-z$ = empirical parameters (with superscript index)
c = concentration
d = diameter
D = diffusion coefficient
F = gas/liquid interfacial area
I = rate of hydrogen dissolution
J = flow to the external catalyst surface
k = rate constant
m = mass
M = molecular weight
n = stirring speed
p = parachor (eq 12)
W = motor power
P = pressure
R = radius of the catalyst particle
Re = Reynolds dimensionless number
S = surface area
Sc = Schmidt dimensionless number
Sh = Sherwood dimensionless number
T = temperature
V = volume
V_λ = relative velocity field
V^* = pure-component volume constant
$V_R^{(0)}$, $V_R^{(\delta)}$ = variables in eq 27

Greek Symbols

β = mass-transfer coefficient
Δ = difference
ϵ = specific mixing power
η = viscosity
η_{eff} = effectiveness factor
η_{SR} = viscosity (the Sastri method)
ι = constant in eq 30
λ = length scale
ν = kinematic viscosity
ξ = catalyst porosity
ρ = density
φ = Thiele modulus
σ = surface tension
τ = time
ϕ = association factor
κ = parameter in eq 18
Φ_G = gas volume fraction in the suspension
χ = catalyst tortuosity
ψ = parameter in eq 28
ω = acentric factor

Subscripts

A, B = components, usually A solvent, B solute
BA = benzoic acid
av = average
b = boiling
bu = bubbles
c = critical
cat = catalyst
eff = efective
eq = equilibrium
G = gas
L = liquid
max = maximum
p = particles
r = reduced
s = saturated
S = solid
vp = vapor

Superscripts

° = infinite dilution
′ = index of empirical parameters
* = index of empirical parameters

Literature Cited

(1) Roberts, G. N. *Catalysis in Organic Chemistry*; Academic Press: New York, 1976.

(2) Santacesaria, E. Kinetics and transport phenomena in heterogeneous gas−solid and gas−liquid−solid systems. *Catal. Today* **1997**, *34*, 411.

(3) Forni, L. Mass and heat transfer in catalytic reactions. *Catal. Today* **1999**, *52*, 147.

(4) Mills, P. L.; Chaudhari, R. V. Multiphase catalytic reactor engineering and design for pharmaceuticals and fine chemicals. *Catal. Today* **1997**, *37*, 367.

(5) Leon, A. Greenberg, L. A.; Lester, D.; Haggard, H. W. *Handbook of Cosmetic Materials*; Interscience Publishers: New York, 1954.

(6) Bedoikian, P. Z. *Perfumery Synthetics and Isolates*; D. Van Nostrand Company: New York, 1951.

(7) Shephard, H. H. *The Chemistry and Action of Insecticides*; McGraw-Hill: New York, 1951.

(8) Cram, D. J.; Hammond, G. S. *Organic Chemistry*; McGraw-Hill: New York, 1964.

(9) Hickingbottom, W. J. *Reactions of Organic Compounds*; Longmans: New York, 1950.

(10) Finar, I. L. *Organic Chemistry*; Longmans: New York, 1951.

(11) Gallezot, P.; Richard, D. Selective hydrogenation of α,β-unsaturated aldehydes. *Catal. Rev.−Sci. Eng.* **1998**, *40*, 81.

(12) Neri, G.; Bonaccorsi, L.; Mercadante, L.; Galvagno, S. Kinetic analysis of cinnamaldehyde hydrogenation over alumina-supported ruthenium catalysts. *Ind. Eng. Chem. Res.* **1997**, *36*, 3554.

(13) Coq, B.; Kumbhar, P. S.; Moreau, C.; Moreau, P.; Warawdekar, M. G. Liquid-phase hydrogenation of cinnamaldehyde over supported ruthenium catalysts: influence of particle size, bimetallics and nature of support. *J. Mol. Catal.* **1993**, *85*, 215.

(14) Neri, G.; Mercadante, L.; Milone, C.; Pietropaolo, R.; Galvagno, S. Hydrogenation of citral and cinnamaldehyde over bimetallic Ru-Me/Al_2O_3 catalysts. *J. Mol. Catal.* **1996**, *108*, 41.

(15) Coq, B.; Kumbhar, P. S.; Moreau, C.; Moreau, P.; Figueras, F. Zirconia-supported monometallic Ru and bimetallic Ru−Sn, Ru−Fe catalysts: Role of metal support interaction in the hydrogenation of cinnamaldehyde. *J. Phys. Chem.* **1994**, *98*, 10180.

(16) Coloma, F.; Sepulveda-Escribano, A.; Fierro, J. L. G.; Rodriguez-Reinoso, F. Crotonaldehyde hydrogenation over bimetallic Pt−Sn catalysts supported on pregraphitized carbon black. Effect of the preparation method. *Appl. Catal.* **1996**, *136*, 231.

(17) Kluson, P.; Cerveny, L. Selective hydrogenation over ruthenium catalysts. *Appl. Catal.* **1995**, *128*, 13.

(18) Neri, G.; Milone, C.; Donato, A.; Mercadante, L.; Visco, A. J. Selective hydrogenation of citral over Pt−Sn supported on activated carbon. *Chem. Technol. Biotechnol.* **1994**, *60*, 83.

(19) Claus, P. Selective hydrogenation of α,β-unsaturated aldehydes and other C═O and C═C bonds containing compounds. *Top. Catal.* **1998**, *5*, 51.

(20) Coq, B.; Kumbhar, P. S.; Moreau, C.; Moreau, P.; Warawdekar, M. G. Liquid-phase hydrogenation of cinnamaldehyde over supported ruthenium catalysts: influence of particle size, bimetallics and nature of support. *J. Mol. Catal.* **1993**, *85*, 215.

(21) Papoutsi, D.; Lianos, P.; Koutsoukos, P. Sol−gel derived TiO_2 microemulsion gels and coatings. *Langmuir* **1994**, *10*, 1684.

(22) Ishii, K.; Mizukami, F.; Niwab, S.; Kutsuzawa, R.; Toba, M.; Fujii, Y. A new catalyst preparation by a combination of complexing agent-assisted sol−gel and impregnation methods. *Catal. Lett.* **1998**, *52*, 49.

(23) Lambert, C. K.; Gonzalez, R. D. The importance of measuring the metal content of supported metal catalysts prepared by the sol−gel method. *Appl. Catal.* **1998**, *172*, 233.

(24) Ward, D. A.; Ko, E. I. Preparing catalytic materials by the sol−gel method. *Ind. Eng. Chem. Res.* **1995**, *34*, 421.

(25) Hajek, J.; Kumar, N.; Salmi, T.; Murzin, D. Yu.; Karhu, H.; Vaeyrynen, J.; Cerveny, L.; Paseka, I. Impact of catalyst reduction mode on selective Hydrogenation of Cinnamaldehyde over Ru−Sn Sol−Gel Catalysts. *Ind. Eng. Chem. Res.* **2003**, *42*, 295.

(26) Hajek, J.; Kumar, N.; Karhu, H.; Cerveny, L.; Vayrynen, J.; Salmi, T.; Murzin, D. Yu. Preparation and properties of bimetallic Ru−Sn sol−gel catalysts: influence of catalyst reduction. *Stud. Surf. Sci. Catal.* **2002**, *143*, 757.

(27) Kolmogorov, A. N. Dissipation of energy in locally isotropic turbulence. *C. R. Dokl. Acad. Sci. URSS* **1941**, *32*, 16.

(28) Temkin, M. I. Transfer of dissolved matter between a turbulently moving liquid and particles suspended in it. *Kinet. Katal.* **1977**, *18*, 493.

(29) Murzin, D. Yu.; Konyukhov, V. Yu.; Kul'kova, N. V.; Temkin, M. I. Diffusion from the surface of suspended particles and specific power of mixing in vibrating reactors. *Kinet. Katal.* **1992**, *33*, 728.

(30) Baldi, G.; Conti, R.; Alaria, E. Complete suspension of particles in mechanically agitated vessels. *Chem. Eng. Sci.* **1978**, *33*, 21.

(31) Reid, R. C.; Prausnitz, J. M.; Poling, B. E. *The Properties of Gases and Liquids*; McGraw-Hill: New York, 1988.

(32) Poling, B. E.; Prausnitz, J. M.; O'Connell, J. P. *The Properties of Gases and Liquids*; McGraw-Hill: New York, 2001.

(33) Murzin, D. Yu.; Kul'kova, N. V. Effect of mass transfer on the kinetics of liquid-phase hydrogenation of organic compounds. *Khim. Prom-st.* **1992**, *11*, 635.

(34) Temkin, M. I. Mathematical modelling and optimization of liquid-phase chemical processes. *Proceedings of Republic Seminar*; VINITI: Moscow, 1987; p 4.

(35) Brunner, E. Solubility of hydrogen in alcohols. *Ber. Bunsen-Ges. Phys. Chem.* **1979**, *83*, 715.

(36) Augustine, R. L. *Heterogeneous Catalysis for the Synthetic Chemist;* Dekker: New York, 1995.

(37) Thiele, E. W. Relation between catalytic activity and size of particle. *J. Ind. Eng. Chem.* **1939**, *31*, 916.

(38) Zel'dovich, Ya. B. The theory of reactions on powders and porous substances. *Acta Physicochim. URSS* **1939**, *10*, 583.

(39) Kapteijn, F.; Marin, G. B.; Moulijn, J. A. Catalytic reaction engineering. *Stud. Surf. Sci. Catal.* **1999**, *123*, 375.

(40) Koo-amornpattana, W.; Winterbottom, J. M. Pt and Pt-alloy catalysts and their properties for the liquid-phase hydrogenation of cinnamaldehyde. 3rd International Symposium on Catalysis in Multiphase Reactors, Naples, Italy, May 29−31, 2000.

Received for review August 20, 2003
Revised manuscript received December 30, 2003
Accepted January 20, 2004

IE0340802